Published in the Proceedings of the 16th International Aluminum Alloys Conference (ICAA16) 2018
ISBN: 978-1-926872-41-4
by the Canadian Institute of Mining, Metallurgy & Petroleum

INFLUENCE OF COOLING RATES ON MICROSTRUCTURE AND Mn SUPERSATURATION IN HIGH-SPEED TWIN-ROLL CAST Al-Mn BASED ALLOY STRIPS

[*]Ram Song, Kazuho Otsuka, Yohei Harada, and Shinji Kumai

Tokyo Institute of Technology
2-12-1 Ookayama, Meguro-ku, Tokyo, Japan
*(*Corresponding author: song.r.aa@m.titech.ac.jp)*

ABSTRACT

Recently, vertical-type high-speed twin-roll casting (HSTRC) has been developed. The HSTRC shows extremely high cooling rates over 1,000 K/s even at the mid-thickness area. The fabricated strip has many metallurgical characteristics; super-saturation of alloying elements, fine solidified structure, and homogeneous distribution of fine constituent particles. In Al-Mn based alloys, the Mn alloying element can be supersaturated in the α-Al matrix and also form Mn-containing constituent particles during solidification. The Mn supersaturation and the distribution of primary/secondary particles in cast products affect the metallurgical behavior in the down-stream processing and can improve mechanical properties of the final products. In this study, Al-Mn based alloy strips were fabricated by HSTRC with various Mn contents. The solidified microstructure, constituent particles and its distribution, and Mn solubility were investigated in the as-cast condition. Due to the high cooling rate of HSTRC, fine constituent particles were homogeneously distributed, and coarse intermetallics were not observed. Mn solid solubility was estimated by electrical conductivity. The estimated Mn solubility was equivalent between strip surface and mid-thickness area.

KEYWORDS

Al-Mn based alloy, High-speed twin-roll casting, Mn solubility, Constituent particle

INTRODUCTION

Al-Mn based alloys, as non-heat treatable wrought aluminum alloys, are widely used in packaging and heat exchanger for automobile industry. Besides Mn, Al-Mn based alloys often contain Fe and/or Si as alloying elements or natural impurities. During solidification , Mn can be super-saturated in the Al matrix, and also form Mn-containing constituent particles. Additionally, in the subsequent thermal-mechanical processes such as homogenization, rolling, and intermediate annealing, Mn in solid solution precipitates out of the Al matrix as secondary particles. The size, distribution, type, and the amount of dispersoids including constituent particles affect to texture evolution, recrystallization behavior, and final mechanical properties of wrought Al-Mn based alloys (Huang et al., 2016; Huang & Marthinsen, 2015; Engler et al., 1995; Muggerud et al., 2013). Therefore, controlling the initial level of Mn super-saturation and the distribution of constituent particles are important in the cast Al-Mn based alloys.

Twin-roll casting (TRC) can be applied for producing an aluminum alloy sheet from the molten metal directly. The TRC can conduct casting and hot rolling in a single step. This provides some advantages such as low fabrication cost, and energy saving compared to other process like direct chill (DC) casting with hot- and cold rolling. Horizontal-type TRC has been popular and widely used for sheet production. In addition to that, recently, vertical-type high-speed twin-roll casting (HSTRC) has been developed with much higher casting speed rather than the conventional horizontal-type TRC. The HSTRC can be carried out at rates of faster than 60 m/min. Extremely high cooling rate over 10^3 K/s was also obtained even at the mid-center area of the as-cast strip (Kim et al., 2010; Song et al., 2018). This feature helps attain get high solid solubility in matrix and homogeneous distribution of secondary particles. The characteristics of HSTRC can expand Mn super-saturation and promote refined secondary particles as well as their homogeneous distribution. Thus, the HSTRC has a high potential to control the microstructure and improve final mechanical properties of Al-Mn based alloy. In the present study, Al-Mn binary and Al-Mn-Fe ternary alloys strips with various Mn contents were fabricated by HSTRC and Mn solubility and microstructural characteristics including constituent particle distribution in the as-cast condition were intensively examined.

EXPERIMENTAL

Various Al-Mn binary and Al-Mn-Fe ternary alloys were used in this study. Al-Mn binary alloys were obtained by melting pure aluminum (99.9 wt%Al) and Al-9.91%Mn alloy. The Mn composition in each binary alloy was 1, 2 and 4 in wt%. Al-Mn-Fe ternary alloys were also prepared by mixing an ingot of Al-1.2%Mn-1%Fe and Al-9.91%Mn alloy. Nominal composition of the each alloys is listed in Table 1.

Table 1. Chemical composition of cast alloys

Alloy	AM1	AM2	AM4	AM1F1	AM2F1	AM3F1
Mn (wt%)	1.0	1.9	4.0	1.2	1.9	3.0
Fe (wt%)	0.1	0.1	0.1	1.0	0.9	0.8
Al	Bal.	Bal.	Bal.	Bal.	Bal.	Bal.

Figure 1 shows a schematic of high-speed twin-roll caster. The roll diameter and width were 300 mm and 100 mm, respectively. Pouring the melts into the caster, solidification shells were formed on the both roll surfaces. The feeding nozzle which was set on the rolls contributes to maintaining stable melt-height. The stable melt-height is necessary for the stable formation of solidification shells on the both roll surfaces. Following rolls rotation, the solidified shells encountered at the roll gap, and were rapidly cooled. At last, a several meters-long thin metal strip was produced within few seconds. Important casting parameters in HSTRC, among others, are casting temperature, roll rotation speed, solidification length (contact length between roll and melt), applied spring load, and initial roll gap. The casting conditions for each alloy are summarized in Table 2.

Approximately 3–4 m long and 100 mm wide strip was fabricated by pouring about 2.5 kg of molten alloy. The strip thickness was measured for middle part of the strip. The constant thickness was obtained in the

middle part of the cast strip (around 1 to 2 m long along the casting direction). The strip thickness was about 2–2.2 mm. It should be noted that microstructure observations made for the part were with the constant thickness. The solidified structure and constituent particle distribution were mainly investigated for the longitudinal cross-section of the as-cast strip. The electrical conductivity was measured by eddy current method at room temperature. For convenience, the electrical conductivity is expressed in terms of %IACS (International Annealed Copper Standard) here. The measured areas were surface and mid-thickness area of the as-cast strip. Generally, the electrical conductivity has linear relationship with electrical resistivity. Thus, the measured electrical conductivity was converted to Mn content in solid solution by using Eq. (1) (Komatsu & Fujikawa, 1997):

$$\text{Mn (wt\%)} = (\rho_{measure} - \rho_{Al})/\ \Delta\rho_{Mn\ in\ Al\ alloy} \quad (1)$$

where $\rho_{measure}$ is the electrical resistivity of each alloy converted by measured electrical conductivity, ρ_{Al} is the electrical resistivity of pure aluminum, $\Delta\rho_{Mn\ in\ Al\ alloy}$ is the electrical resistivity contribution for Mn element in Al matrix. The electrical resistivity of pure aluminum, ρ_{Al} is 26.5 nΩm, and the electrical resistivity contribution of Mn element, $\Delta\rho_{Mn\ in\ Al\ alloy}$ is 31 nΩm wt%$^{-1}$ at room temperature. The electrical conductivity change is influenced by the amount of dissolved alloying elements in the Al matrix. In the case of Al-Mn-Fe ternary alloy, the solubility of Fe in Al matrix is quite low. Thus, the electrical conductivity change is considered to be mainly due to the variation of Mn in solid solution.

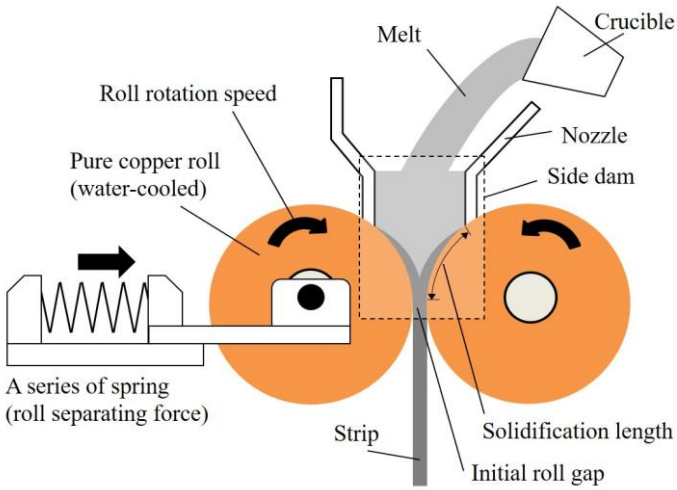

Figure 1. Schematic diagram of the high-speed twin-roll caster

Table 2. HSTRC condition of each alloy strip

Condition	Alloy					
	AM1	AM2	AM4	AM1F1	AM2F1	AM3F1
Casting temperature (K)	948	948	1053	953	953	1008
Roll rotation speed (mm/min)	60	60	60	60	60	60
Solidification length (mm)	100	100	100	100	100	100
Applied spring load (kN)	20	20	60	20	20	40
Initial roll gap (mm)	1	1	0.8	1	1	1

RESULTS

Mn Solubility Estimation by Electrical Conductivity

The electrical conductivity and corresponding Mn solubility estimation are summarized in Table 3. Each as-cast strip showed equivalent Mn solubility in both surface and mid-thickness area. In the Al-Mn binary alloys, estimated Mn solubility was almost idential to the alloy composition for Al-1, 2 wt% Mn strip, while a slightly lower content was obtained for Al-4wt% Mn alloy. In the Al-Mn-Fe ternary alloys, estimated Mn solubility was lower than the alloy composition. Compared to AM2F1 and AM3F1, there was no large difference, around 1.4–1.6 in Mn content.

Table 3. Electrical conductivity and estimated Mn solubility in Al-Mn based alloys strip

Alloy	AM1		AM2		AM4		AM1F1		AM2F1		AM3F1	
Position	Sur.	Cen.	Sur.	Cen.	Sur.	Cen.	Sur.	Cen.	Sur.	Cen.	Sur.	Cen.
%IACS	27.1	28.5	19.3	19.3	12.5	12.0	30.6	30.3	24.0	24.3	22.3	23.3
Mn (wt%)	1.19	1.10	2.02	2.02	3.59	3.78	0.95	0.98	1.46	1.43	1.64	1.53

Strip Macrostructure

Figure 2 shows representative macroscopic-view of the grain structure in the cross-section of as-cast Al-Mn binary and Al-Mn-Fe ternary alloy strip. During the pouring of the melts into the high-speed twin-roll caster, the melt contacted with the roll surface was raipdly cooled. Chilled areas are observed at the strip surface. Along the thickness direction of the strip, there were columnar grains grown from the both surfaces, then they encountered at the mid-thickness area in the Al-Mn binary alloy strip as shown in Figure 2(a). This is similar to that of pure Al strip (Kim et al., 2010). In the Al-Mn-Fe ternary alloy strip, the chilled areas were also observed at the strip surface. The solidified shells were formed and grew on the both roll surfaces. This area was filled with fine columnar grains. In contrast, equiaxed grains were observed in mid-thickness area as shown in Figure 2(b). The band thickness of equiaxed grains was irregular along the transverse and longitudinal directions.

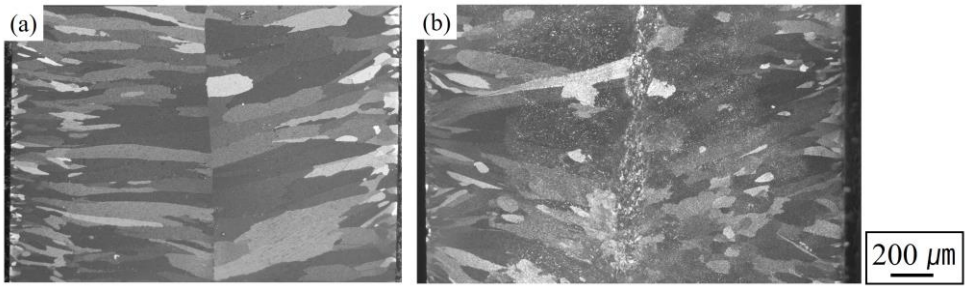

Figure 2. Representative macrostructure of the cross-section of strip. (a) is AM2 alloy strip, (b) is AM2F1 alloy strip

Strip Microstructure

Figure 3 shows representative microstructures of the cross-section at mid-thickness of as-cast Al-Mn binary and Al-Mn-Fe ternary alloy strip. The distribution of constituent particles can be recognized by that of etched pits. In AM2 alloy strip, celllular and columnar dendritic structure were observed. As shown in Figure 3(a), solidified shells grew to the strip center. Coarse Al-Mn intermetallic compounds were hardly observed on both strip surface and center. In contrast, AM2F1 alloy strip showed clearly different microstructure along the thickness direction. Near surface, very fine cell structure was observed (Figure 3(c)), and it changed into fine dendritic structure (Figure 3(d)). Due to low solubility of Fe in Al matrix, Fe-containing intermetallics were located in the inter-cellular areas as well as grain boundaries. In mid-thickness area, some primary intermetallic particles were observed as shown in Figure 3(e).

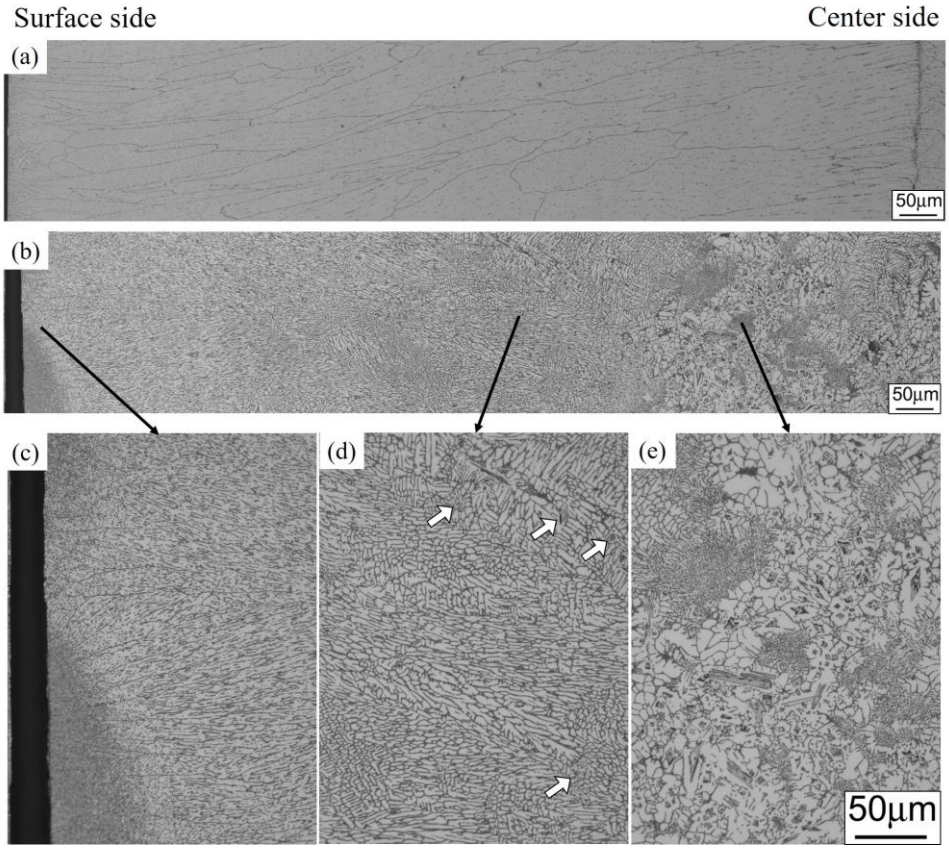

Figure 3. Typical microstructure of the cross-section of strip. (a) is AM2 alloy strip, (b) is AM2F1 alloy strip (c),(d),(e) are details of specific areas in (b)

DISCUSSION

Influence of Cooling Rate on Mn Solubility

There were no specific difference in estimated Mn solubility between strip surface and mid-thickness area in as-cast strip. The Mn solubility can be influenced by casting parameters; casting temperature, spring force which affects the cooling rate during the casting. It is known that the cooling rate of HSTRC is over 10^3 K/s (Kim et al., 2010; Song et al., 2018). This high cooling rate contributes to result in not only equivalent Mn solubility along thickness of the strip, but also high Mn supersaturation over 3.5 wt% in Al-Mn binary alloy. In Al-Mn-Fe ternary alloy, a large amount of Mn- and Fe- containing constituent particles can be formed during solidification due to the low solubility of Fe in Al matrix. This may cause the drastic reduction of Mn solubility in Al matrix rather than Al-Mn binary alloy. Compared to AM1 binary alloy, AM1F1 showed equivalent Mn solubility in the Al matrix. It means that around 1 wt% concentration of Mn in solid solution is feasible even in the Al-Mn-Fe ternary alloy. With increasing Mn content, the estimated Mn solubility was basically 1.5 wt% even in AM3F1 alloy. This suggests that the high cooling rate of the HSTRC enhanced Mn supersaturation in as-cast condition effectively even in the ternary alloy system that forms Mn-containing constituent particles during solidification.

Constituent Particle Distribution in As-Cast Strip

Due to the high cooling rate of the HSTRC, fine primary α-Al dendrites were observed near the strip surface. The constituent particles are normally found in the vicinity of grain boundaries. In the Al-Mn binary alloy, most of the Mn was supersaturated in Al matrix as a solute. Thus, intermetallic particles were hardly

observed in AM2 alloy strip as shown in Figure 3(a). By refinement of α-Al dendrites due to high cooling rate of HSTRC, Fe-containing intermetallics were also refined which were located in the inter-cellular areas as well as grain boundaries in the Al-Mn-Fe ternary alloy strip as shown in Figure 3(c).

As shown in Figure 3(e), some relatively-large intermetallic compounds were observed at mid-thickness area. Their size and morphology were different from those of particles at inter-cellular areas. Meanwhile, the direct temperature measurement revealed that the cooling rate is considered more than 10^3 K/s even at the center of strip (Kim et al., 2010; Song et al., 2018). It is hard to consider that large intermetallic compounds formed at such high cooling rate during solidification. Also, in Al-Mn-Fe alloys, primary phase is considered not α-Al solid solution, but Fe-containing intermetallics. Therefore, the large intermetallic particles were considered as primary intermetallics formed in the melt pool. Floating intermetallic particles can be trapped by growing solidification shells (marked in Figure 3(d)), or can be pushed to the mid-central region by the growing solid fronts. Even though the applied casting temperature was higher than liquidus temperature of those alloys, primary intermetallic particles can be formed in the melt pool. However, considering the casting speed, the entire process from the melts to as-cast strip was finished within few seconds. Thus, coarse primary intermetallic particles were not formed in as-cast strip.

CONCLUSIONS

Enhancement of Mn solubility in Al matrix was obtained due to the high cooling effect of high-speed twin-roll casting. The estimated Mn solubility was over 3.5wt% Mn in the Al-Mn binary alloy. It was around 1.5wt% Mn in solid solution even in the Al-Mn-Fe ternary alloy. Refinement of constituent particles was also confirmed. Intermetallic particles were hardly observed in Al-Mn binary alloy strip. Also, coarse primary intermetallic particles were not formed in Al-Mn-Fe ternary alloy strip.

REFERENCES

Huang, K., Logé, R.E. & Marthinsen, K. (2016). On the sluggish recrystallization of a cold-rolled Al-Mn-Fe-Si alloy. *Journal of Materials Science*, *51*(3), 1632-1643. https://doi.org/10.1007/s10853-015-9486-y

Huang, K. & Marthinsen, K. (2015). The effect of heating rate on the softening behaviour of a deformed Al-Mn alloy with strong and weak concurrent precipitation. *Materials Characterization*, *11*0, 215-221. https://doi.org/10.1016/j.matchar.2015.10.033

Engler, O. Yang, P. & Kong, X.W. (1995). On the formation of recrystallization textures in binary Al-1.3% Mn investigated by means of local texture analysis. *Acta Metallurgica*, *44*(8), 3349-3369. https://doi.org/10.1016/1359-6454(95)00416-5

Muggerud, A.M.F., Mø.rtsell, E.A., Li, Y.J. & Holmestad, R. (2013). Dispersoid strengthening in AA3xxx alloys with varying Mn and Si content during annealing at low temperatures. *Materials Science & Engineering A*, *567*(1), 21-28. https://doi.org/10.1016/j.msea.2013.01.004

Komatsu, S. & Fujikawa, S. (1997). Electrical resistivity of light metals and alloys-Its measurement, interpretation and application Part1 Methodology and basic values. *Journal of Japan Institute Light Metals*, *47*(4), 170-181. http://doi.org/10.2464/jilm.47.170

Kim, M.S., Arai, Y., Hori, Y. & Kumai, S. (2010). Formation of internal crack in high-speed twin-roll cast 6022 aluminum alloy strip. *Materials Transactions*, *51*(10), 1854-1860. https://doi.org/10.2320/matertrans.L-M2010818

Song, R., Harada, Y. & Kumai, S. (2018). Influence of cooling rate on primary particle and solute distribution in high-speed twin-roll cast Al-Mn based alloy strip. *Materials Transactions*, *59*(1), 110-116. https://doi.org/10.2320/matertrans.F-M2017843